The vestibulospinal nucleus is a locus of balance development

Kyla R. Hamling[1], Katherine Harmon[1], Yukiko Kimura[2], Shin-ichi Higashijima[2], David Schoppik[1]
[1] Departments of Otolaryngology, Neuroscience & Physiology, and the Neuroscience Institute, New York University Grossman School of Medicine
[2] National Institutes of Natural Sciences, Exploratory Research Center on Life and Living Systems (ExCELLS), National Institute for Basic Biology, Okazaki 444-8787, Aichi, Japan
Correspondence: schoppik@gmail.com

ABSTRACT

Mature vertebrates maintain posture using vestibulospinal neurons that transform sensed instability into reflexive commands to spinal motor circuits. Postural stability improves across development. However, due to the complexity of terrestrial locomotion, vestibulospinal contributions to postural refinement in early life remain unexplored. Here we leveraged the relative simplicity of underwater locomotion to quantify the postural consequences of losing vestibulospinal neurons during development in larval zebrafish. By comparing posture at two timepoints, we discovered that later lesions of vestibulospinal neurons led to greater instability. Analysis of thousands of individual swim bouts revealed that lesions disrupted movement timing and corrective reflexes without impacting swim kinematics, particularly in older larvae. Using a generative model of swimming, we showed how these disruptions could account for the increased postural variability at both timepoints. Finally, late lesions disrupted the fin/trunk coordination observed in older larvae, linking vestibulospinal neurons to postural control schemes used to navigate in depth. Since later lesions were considerably more disruptive to postural stability, we conclude that vestibulospinal contributions to balance increase as larvae mature. Vestibulospinal neurons are highly conserved across vertebrates; we therefore propose that they are a substrate for developmental improvements to postural control.

INTRODUCTION

Animals actively modulate the timing and strength of their trunk and limb movements to remain balanced during locomotion [1–5]. In many species, balance control improves during early postnatal life as the behavioral strategies to correct imbalance develop and refine. Understanding these sensorimotor computations, and how they refine over time, requires identifying the neurons that contribute towards balance development. Vestibulospinal neurons are descending projection neurons conserved across vertebrates that are well-poised to regulate balance [6–12]. They have somata in the lateral vestibular nucleus [13,14] and receive convergent excitatory [15,16] and inhibitory vestibular input [17,18] as well as a wide variety of extravestibular inputs [19].

Vestibulospinal neuron function and their precise contribution to behavior remain active areas of research. However, the complexity of the mammalian nervous system and of tetrapod locomotion constrain progress. In decerebrate cats, vestibulospinal neurons encode body tilts, are active during extensor muscle contraction during locomotion [16,20–22], and relay VIIIth nerve activity to ipsilateral extensor muscles [23,24]. Recent technological improvements permit targeting of genetically-defined populations of vestibulospinal neurons in mice. Loss of function experiments using these tools established that vestibulospinal neurons are necessary for specific hindlimb extension reflexes in response to imposed instability [25,26]. Questions remain as to whether vestibulospinal neurons play a role in balance control outside of their effect on hindlimb extension, what role they might play in balance control during natural movement, and whether their role changes as balance matures.

Swimming offers a particularly tractable means to assay neuronal contributions to balance computations, especially across development. The biophysical and biomechanical contributions to swimming are straightforward to delineate [27,28]. For example, larval zebrafish swim with short discontinuous propulsive movements called “bouts” that constitute active locomotion. Between bouts, they are passive, akin to standing still. This dichotomy allows for dissociation of passive and active (i.e. neuronal) contributions to stability. Larval zebrafish maintain their preferred near-horizontal pitch using two active computations: they initiate swim bouts to occur when pitched off-balance and they rotate their bodies during bouts to restore posture [29–31]. Similar corrections stabilize posture in the roll axis [32]. Importantly, both behaviors improve over the first week of life [29–31].

Vestibulospinal neurons are a promising candidate substrate for vertebrate postural development. Vestibulospinal pathways are highly-conserved between mammals and teleost fish, sharing similar anatomy [11,33,34], developmental ontology [35], and functional responses [36,37]. In mammals, vestibulospinal pathways are formed and have functional synapses by birth [38]. Experiments in mice show that loss of vestibulospinal pathways can affect vestibular hindlimb reflexes in pups, supporting an early behavioral role for this circuit [25]. In larval zebrafish, vestibulospinal neurons can encode vestibular stimuli as early as 4 days post-fertilization (dpf) [34,36,37], as they receive a rich complement of sensory inputs from the inner ear [39,40]. In addition, the refinement of posture-related behaviors in larval fish likely involves central vestibular circuits, as loss of the vestibular periphery disrupts trunk/fin coordination that larval zebrafish learn to use during early life to climb in depth [41]. The early engagement of this evolutionarily-conserved circuit supports using the larval zebrafish to investigate the role of vestibulospinal neurons in balance development.

Here, we adopted a loss-of-function approach to define the role of vestibulospinal neurons to postural orientation in freely swimming fish during early development. We selected two important timepoints: 4 days post-fertilization (dpf),

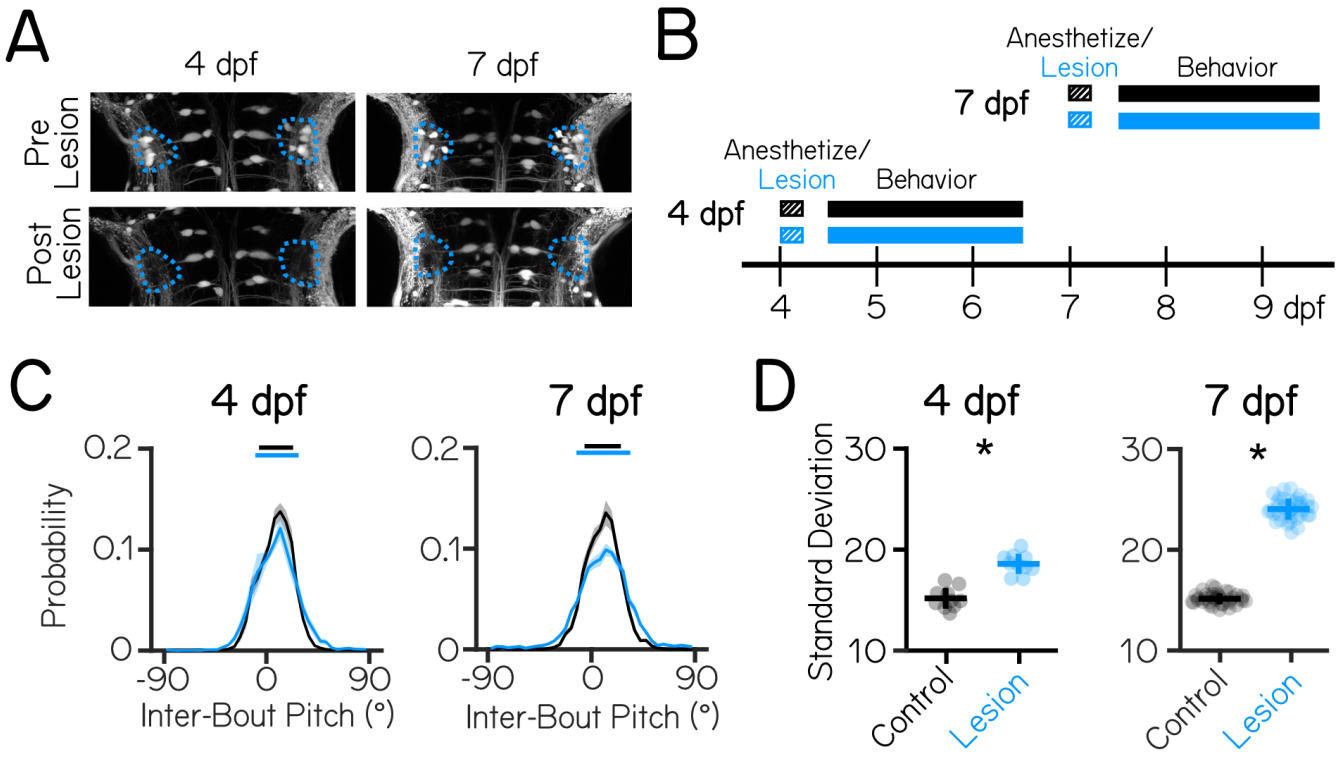

Figure 1: Vestibulospinal neurons contribute to postural stability with increasing effects in older fish.
(A) Images taken before and after targeted photoablations of genetically-labeled vestibulospinal neurons show selective loss of fluorescent somata in outlined area (blue) at lesions performed at either 4 dpf (left), or 7 dpf (right).
(B) Timeline of the experimental strategy. Fish were either vestibulospinal-lesioned (blue) or non-lesioned sibling controls (black) that were allowed to recover for 4 hours post-lesion and then assayed for postural behavior for 48 hours. Separate experiments were run for fish assayed with lesions at 4 dpf or lesions at 7 dpf.
(C) Distributions of observed pitch show no change to average posture (dashed vertical lines) but greater variability (solid horizontal lines ± 1 SD) between control fish (black) and lesioned siblings (blue)
(D) Postural variability (standard deviation of pitch) is greater in lesioned fish than sibling controls; lines are jackknifed mean ± standard deviation. Asterisks represent statistically significant differences, $p<0.05$.

when fish begin to orient and swim freely, and 7 dpf, after key stabilizing computations have matured. After targeted lesions of vestibulospinal neurons, fish could still swim and continued to orient and navigate in depth. Posture was more variable after lesions at both timepoints, and this effect was considerably more pronounced at 7 than at 4 dpf. Analysis of individual swim bouts revealed that loss of vestibulospinal neurons disrupted posture-dependent bout initiation and restorative rotations; the effects of the lesion increased at 7 dpf. We used a model of swimming to determine that such disruptions could account for the increased postural variability we observed at both ages. Finally, we found that coordination of fin and body effectors was impaired after vestibulospinal loss at 7, but not 4 dpf. Altogether, our work determines the specific contribution of vestibulospinal neurons to computations that stabilize posture and facilitate vertical navigation across early development. Given the near-ubiquity of vestibulospinal neurons across vertebrates, and the shared challenge of postural development, we propose that this circuit may serve as a substrate for developmental improvements to balance.

RESULTS

Loss of vestibulospinal neurons at 7 dpf disrupts postural stability more strongly than 4 dpf

Previous electrophysiological[34,36] and imaging[37] studies indicate that the larval zebrafish vestibulospinal circuit is poised to regulate posture by encoding body tilt and translation. To determine the specific vestibulospinal contributions to postural stability, we adopted a loss-of-function approach. The transgenic line *Tg(nefma::EGFP)*, reliably labels 30±6 vestibulospinal neurons per brain hemisphere (61% of the total population, Figure S1A). We could routinely ablate the majority of labelled neurons (22±4 neurons at 4 dpf, 23±5 neurons at 7 dpf) without damaging surrounding neurons or neuropil (Figure 1A). Photoablated neurons remained absent from larvae 3 days after the lesion occurred suggesting no vestibulospinal recovery or regeneration occurred (1.7±1.5 neurons labelled by spinal backfill in lesioned hemisphere vs 14.7±2.4 in control hemisphere; paired t-test $p=1.7x10^{-6}$).

We used an automated machine vision-based assay[29,31] to measure locomotion and posture in the pitch axis (nose-up/nose-down) as larvae swam freely in the dark. We measured swim-related kinematics, and postures adopted in between swim bouts. We performed lesions at either 4 or 7 dpf, and monitored locomotion and posture for a 48 hour period after a 4 hour post-lesion recovery period (Figure 1B) (n = 5 clutch replicates lesions, 54 lesioned fish and 54

lesioned control siblings at 4 dpf; n = 9 clutch replicates, 97 lesioned fish and 76 control siblings at 7 dpf).

We first examined whether loss of vestibulospinal neurons at 4 dpf disrupted the ability of larvae to maintain posture. After vestibulospinal lesions, the distribution of inter-bout pitches adopted by the fish was broader (standard deviation of pitch distribution = 15.2±1.0° controls vs 18.6±1.0° lesioned; $p=6.7x10^{-7}$) (Figures 1C and 1D). Lesioned fish were more likely to be found at extreme nose-up or nose-down postures (absolute pitch angle greater than 45°) compared to their siblings (1.1% of inter-bout observations in control vs. 3.0% of lesioned observations) and less likely to be found near (±5°) to their preferred posture (25.8% control vs 21.9% lesioned). However, the preferred postural set point was not affected (mean posture 9.8±4.5° controls vs. 8.5±6.5° lesions p=0.71). As the behavioral assay lasted for 48 hours from 4 to 6 dpf, we reasoned that the effect of the lesion might change across this period if the effect of vestibulospinal loss changed within this time window, or if recovery occurred. We found that the effect of the lesion was similar across the first and second 24 hour period (standard deviation of pitch distribution: 19.1±1.8° 4 dpf Day 1 vs. 18.0±1.0° Day 2, paired t-test p=0.10), suggesting that compensation did not occur after the lesion and that loss of vestibulospinal neurons disrupts stability even at the earliest assayed timepoint. This finding indicates that vestibulospinal neurons contribute functionally towards maintaining stable posture and that this contribution is behaviorally-relevant by 4 dpf.

At 7 dpf, lesioned fish showed more profound disruptions to posture. Lesions at 7dpf had a broader distribution of inter-bout pitches than their control siblings (15.1±0.5° controls vs 24.0±1.0° lesioned; $p=1.4x10^{-53}$, Figures 1C and 1D). The effect of the lesion on the distribution of observed pitches was stronger at 7 dpf than at 4 dpf (Cohen's d effect size = 10.7 at 7 dpf, 3.3 at 4 dpf). While both lesioned and control siblings maintained their posture slightly nose-up from horizontal (mean 9.2±3.9° vs. 9.5±3.6°), lesioned fish are less likely to be found close to their preferred posture (24.6% lesioned vs 17.9% control) and more likely to be found at eccentric nose-up and nose-down postures that control fish rarely adopt (7.5% lesioned vs 1.7% control). Consistent with the results from 4-6 dpf, behavior did not improve across the 48 hour period of the 7 dpf assay (standard deviation of pitch distribution: 23.6±1.2° 7 dpf Day 1 vs 23.7±1.8° Day 2, paired t-test p=0.64).

Lesions at either age did not affect basic kinematic properties such as bout speed, bout duration, or bout frequency (Table 1). Instead, loss of vestibulospinal neurons disrupts the observed distributions of body posture in the pitch axis. Importantly, disruptions to posture are stronger when neurons are lost later in larval development, a key hallmark of a neuronal substrate for balance development.

Vestibulospinal lesions at 7 dpf perturb posture-dependent movement timing and corrective gain computations more than at 4 dpf

Larval zebrafish adopt two behavioral strategies to stabilize posture in the pitch axis. First, translation through the water passively counteracts destabilizing torques[28]. Fish can therefore correct for destabilization by continuously swimming, or by preferentially initiating swim bouts when they sense instability. We previously showed that larvae develop the ability to do the latter[29] and termed this change to bout initiation "pitch sensitivity." Second, as part of each bout, larvae actively make angular rotations that partially restore them to their preferred posture[30,31]. These movements are called "corrective rotations," and their gain (the fraction corrected) increases with age. Together, changes to pitch sensitivity and corrective rotations underlie the development of posture in the pitch axis.

To determine if loss of vestibulospinal neurons interferes with the development of posture, we first assayed pitch sensitivity. The relationship between bout rate and posture is well fit by a parabola (Figure 2A), with two important free parameters: the steepness (pitch sensitivity) and the vertical offset (basal rate of movement). We hypothesized that if vestibulospinal neurons contribute to posture-mediated bout initiation then their loss should (1) flatten this parabola, reflecting decreased pitch sensitivity and (2) increase the basal bout rate to compensate.

At 4 dpf, we found that pitch sensitivity was modestly increased in vestibulospinal lesioned fish (0.18±0.07 mHz/deg^2 controls vs 0.25±0.05 mHz/deg^2 lesioned, p=0.015) (Figure 2B). Basal bout rate was not significantly different between lesions and control (0.74±0.14 Hz controls vs 0.73±0.03 Hz lesions, p=0.82).

In marked contrast, fish lesioned at 7 dpf had decreased pitch sensitivity relative to control siblings (0.41±0.07 controls vs 0.14±0.02 lesioned; $p=4.0x10^{-33}$; Figure 2B). Further, basal bout rate was increased in lesioned fish (0.63±0.03 Hz controls vs 0.77±0.05 Hz lesioned). As lesioned fish had significantly more observations at extreme pitch angles compared to controls, we reasoned that pitch sensitivity could be lower in lesions due to changes to the distribution of pitch. However, we found that the effect of the lesion persisted even after removing the most eccentric pitches (absolute angle above 45°) from the calculation of pitch sensitivity fit (mean pitch sensitivity = 0.47±0.07 mHz/deg^2 controls vs 0.28±0.05 mHz/deg^2 lesioned, $p=3.2x10^{-21}$). We conclude that changes at 7 dpf are not an artefact of the most extreme posture deviations. Finally, consistent with previous findings[29], pitch sensitivity was substantially larger in control larvae when measured at 7 dpf than at 4 dpf (0.18±0.07 mHz/deg^2 4 dpf vs. 0.41±0.07 mHz/deg^2 7 dpf controls). This developmental increase was entirely absent in lesioned fish assayed at 7 dpf (0.25±0.05 mHz/deg^2 4 dpf vs. 0.14±0.02 mHz/deg^2 7 dpf lesioned (Figure 2B).

Fish also modulate swim bout frequency as a function of their angular velocity. To test whether angular velocity sensitivity was affected by vestibulospinal lesions, we fit a line to the relationship between bout rate and angular velocity for both negative (nose-down) and positive (nose-up) angular velocity deviations (Figure S2A). Neither up nor down angular velocity sensitivity changed after vestibulospinal lesions at 4 dpf (angular velocity sensitivity nose-up: 0.10±0.01 lesioned vs 0.10±0.03 controls, p=0.89. Nose-down: -0.07±0.02 lesioned vs -0.08±0.01 controls, p=0.08)(Figures S2B and S2C). At 7 dpf, lesioned fish showed a weaker relationship between bout rate and angular velocity prior to a bout (Nose-up: 0.09±0.01 deg^{-1} lesioned vs 0.12±0.01 deg^{-1} controls, $p=7.5x10^{-17}$; Nose-down: -0.08±0.01 deg^{-1} lesioned

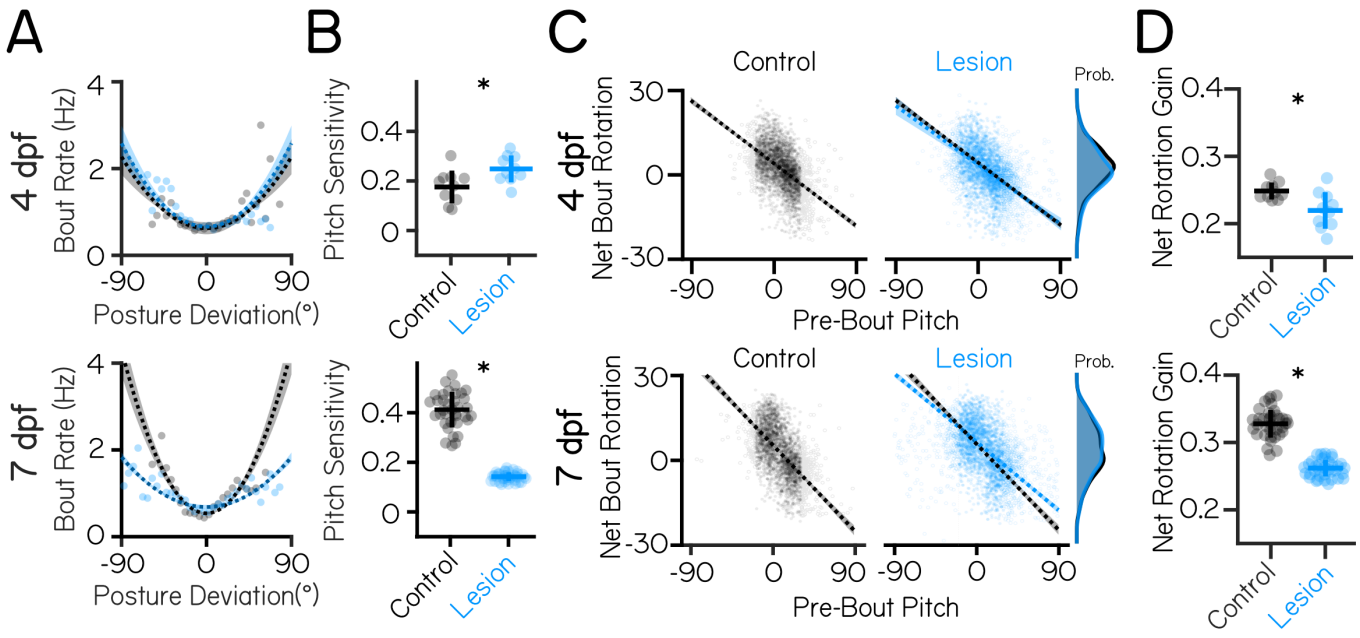

Figure 2: Vestibulospinal neurons contribute to movement timing and corrective capacity with increased effects at 7 dpf than 4 dpf.
(A) Movement timing (bout rate as a function of deviation from preferred posture) in lesioned fish (blue) and sibling controls (black). Dots are means of raw data falling within 5° bins, dashed lines are parabolic fits to raw data ± 1 S.D.
(B) Pitch sensitivity (parabolic steepness between posture deviation and bout rate) in lesioned fish and sibling controls at 4 dpf (top) and 7 dpf (bottom). Lines are jackknifed mean ± 1 SD, dots are jackknifed replicates.
(C) Net bout rotation (change in pitch angle before and after a swim bout) as a function of pre-bout pitch in sibling controls (black, left) and vestibulospinal lesioned fish (blue, right). Filled dots are raw data used for linear fits (between -30 and +20°), outlined dots are raw data exclude from fits due to falling outside of the pitch range that can be well-described by a linear fit. Dashed lines are linear fits to included raw data ± 1 S.D. Control linear fits (black) are replotted onto lesioned fish data for ease of comparison. Probability distributions (far right) show distribution of net bout rotation across pitches.
(D) Bout rotation gain (absolute slope of the linear fit between pre-bout pitch and net bout rotation) decreases in vestibulospinal lesioned fish at both 4 dpf (top) and 7 dpf (bottom). Lines are jackknifed mean ± 1 SD, dots are jackknifed replicates. Asterisks represent statistically significant differences, p<0.05.

vs -0.10±0.01 deg^{-1} controls, p=4.4x10^{-13}) (Figures S2A to S2C). Together, these findings suggest that at 4 dpf vestibulospinal neurons do not contribute towards the increase in movement frequency at unstable pitches/angular velocities but that at 7 dpf, loss of vestibulospinal neurons disrupts the fish's ability to preferentially time their swim movements to their experience of instability both at high pitch angle and angular velocities.

We next assessed whether the second key computation that contributes to pitch stability – the ability to generate corrective rotations during a swim bout – was affected by vestibulospinal lesions. Larval zebrafish experience a counter-rotation during a swim bout that is negatively correlated with their posture before the swim bout [29,31]; the magnitude of this correlation is the "gain" of the pitch correction. In fish with vestibulospinal lesions at 4 dpf, pitch correction gain was lower (0.25±0.01 controls vs 0.22±0.03 lesioned, p=0.007) (Figures 2C and 2D). In fish lesioned at 7 dpf, bouts were also less corrective for pitch instability (pitch correction gain: 0.33±0.02 controls vs 0.26±0.01; p=8.8x10^{-26}) (Figures 2C and 2D).

Importantly, as compared to the effects of the 4 dpf lesion, lesions at 7 dpf had a stronger effect on pitch correction (Cohen's d effect size = 1.36 at 4 dpf, 3.89 at 7 dpf). Similar to the effects on movement timing, we noticed that pitch correction gain increased in control larvae between 4 and 7 dpf (0.25±0.01 at 4 dpf vs. 0.33±0.02 at 7 dpf), and that the gain in 7 dpf lesioned fish was reduced to levels comparable to their behavior at 4 dpf. At both ages lesioned fish performed corrective rotations of comparable magnitudes to those of their control siblings (net rotation 95% intervals:-11°to +14° controls 4 dpf, -13°to +14° lesioned 4 dpf; -12°to +17° controls 7 dpf, -13°to +18° lesioned 7 dpf) (Figure 2C, far right), indicating that lesioned fish are capable of making corrective rotations but do not pair them appropriately to their starting posture. Bouts in lesioned fish also had a small but significant decrease in their capacity to correct for angular velocity instability (Figure S2D) at both 4 and 7 dpf, supporting the idea that vestibulospinal lesion disrupted the corrective nature of bouts.

While vestibulospinal lesions have clear effects on overall postural stability and the specific computations that help maintain posture, lesioned fish still maintain some level of postural control. To determine whether the residual ability to control posture reflected an incomplete lesion, we repeated our experiments at 7 dpf following optical backfill [42] of all spinal-projecting neurons in the *Tg(α-tubulin:C3PA-GFP)* line (Figure S1B). Lesions removed nearly all vestibulospinal neurons (n=42±10 neurons, n=13 fish), yet produced comparable effects on the standard deviation of pitch distribution (13.5° controls vs 20.2° lesions, p=5.5x10^{-9}) and on pitch sensitivity (0.42 controls vs 0.18 lesions; p=9.9x10^{-5}) as

the partial lesions targeted in the *Tg(nefma::EGFP)* background at 7 dpf (Figures S1C to S1F). Lesioned fish also had comparably impaired corrective counter-rotations (pitch correction gain: -0.19 controls vs -0.09 lesions; p=0.007). We propose that the remaining ability to control pitch sensitivity /corrective counter-rotations reflects extra-vestibulospinal contributions to posture.

Taken together, the results of our lesion experiments support the hypothesis that vestibulospinal neurons play a larger role in postural control as fish develop. We observed that vestibulospinal neurons play a role in postural control behavior as early as 4 dpf. Further, the importance of the vestibulospinal circuit towards postural control increases between the first week of development (4-6 dpf) and early in the second week (7-9 dpf). Specifically, our data argue that loss of vestibulospinal neurons increases variability in the pitch axis by interfering with corrective gain at an early developmental age, and posture-dependent movement timing and corrective gain by the second week of larval life.

A computational model of swimming can explain age-specific consequences of vestibulospinal lesion on postural stability

Loss of vestibulospinal neurons leads to instability in the pitch axis, and disrupts key behaviors that correct posture. Are the changes to disrupted bout timing and/or corrective rotations sufficient to explain the observed instability at both 4 and 7 dpf? To determine the postural impact of vestibulospinal neuron loss, we simulated pitch using a generative model of swimming [29] (Figure 3A). Model larvae are subject to passive destabilization that is partially corrected by stochastic swim bouts whose kinematics and timing are drawn from distributions that match empirical observations. Of twenty-one data-derived parameters (Table 2), fifteen implement the two relevant computations: nine that determine the degree to which bout probability depends on either pitch or angular velocity (bout timing) and six that determine the degree to which bouts restore posture (corrective stabilization). Both bout timing and corrective rotations are required to generate simulated bouts with a preferred horizontal posture and a low-variability pitch distribution (Figure S3A), consistent with previous findings [29].

Our model recapitulated the empirical distributions of posture and swim bout timing (Figures S3B to S3D) using parameters derived from control and lesioned data at both 4 and 7 dpf. Modeled pitch distributions had similar mean pitch and standard deviations compared to empirical control data at both 4 dpf (mean posture 9.5±1.3° control model, mean distribution standard deviation 15.5±0.8° control model) and 7 dpf (mean posture 6.8±1.0° control model, mean distribution standard deviation 14.8±0.6° control model). Models of control data captured most of the variability (>98% of empirical standard deviation) seen in the empirical control distribution at 4 and 7 dpf. Relative to controls, models of lesion data showed broader distributions of pitch angles (mean distribution standard deviation 16.4±0.7° lesion 4 dpf model, 19.1±1.9° lesion 7 dpf model). However, our framework underestimates the impact of lesions on posture (88% and 80% of empirical standard deviation from 4 and 7 dpf dataset respectively).

If vestibulospinal lesions impair posture stability through disruptions to bout timing and corrective counter-rotations, then changes to both (but not either alone) should explain the increased variability in posture. Alternatively, if one computation alone is sufficient to account for the increased postural variability, then changes in the other computation may be unrelated to effects on stability after lesion. To test how lesion-driven changes to specific computations relate to changes in pitch stability, we systematically replaced the relevant parameters for each computation with those from lesion data (Figure 3B), resulting in a model that is either derived entirely from control parameters ("Full Control Model", green), entirely from lesion parameters ("Full Lesion Model", blue) or from a mix of control and lesion parameters ("Hybrid Models", gray). We then analyzed the standard deviation of the resulting generated pitch distributions from the full control and full lesion models to the hybrid models.

In the 4 dpf hybrid models, only the model that replaced parameters related to bout correction had a significantly higher standard deviation of pitch compared to the control model (One-Way ANOVA main effect $p=2.5x10^{-13}$, Tukey's post-hoc test $p=2.2x10^{-6}$), and this model was as unstable as the full lesion model (Figure 3C). In contrast, hybrid models based on 7 dpf data, both the model that replaced only bout correction parameters ("Lesion Correction") and the model that replaced bout correction and bout timing parameters together ("Timing + Correction") had significantly higher pitch standard deviation compared to the control model (One-Way ANOVA main effect $p=2.2x10^{-69}$, Tukey's post-hoc test $p=5.9x10^{-8}$), but not the model with just bout timing parameters replaced ("Lesion Timing") (Figure 3D). Alone, neither the Lesion Timing nor the Lesion Correction model recapitulated the variability we observed (Figure 3D). Together, the Timing + Correction hybrid model could (no statistical difference between Full Lesion and Timing + Correction model, Tukey's post-hoc test p=0.9).

Changes to the corrective capacity of swim bouts are sufficient to recapitulate the effect of early (4 dpf) loss of vestibulospinal neurons. However, to effectively model loss of vestibulospinal neurons in older larvae (7 dpf) requires changes to bout timing and corrective gain. Our models therefore support the hypothesis that the contribution of vestibulospinal neurons to balance increases over development.

Vestibulospinal neurons contribute towards coordination of fin use and body posture

Previous work has established a role for vestibulospinal neurons in paired appendage (limb) movement during postural corrections [25,26]. While zebrafish do not have limbs, they do have pectoral fins, a likely evolutionary precursor of mammalian forelimbs [43]. Pectoral fins in larval zebrafish can generate lift that, when coordinated with trunk rotations, helps fish to climb in the water column. These coordinated movements rely on vestibular sensation and improve over development [41]. We hypothesized that vestibulospinal neurons in the larval fish might contribute towards vestibular-driven fin function, as they do in limb function in mammals.

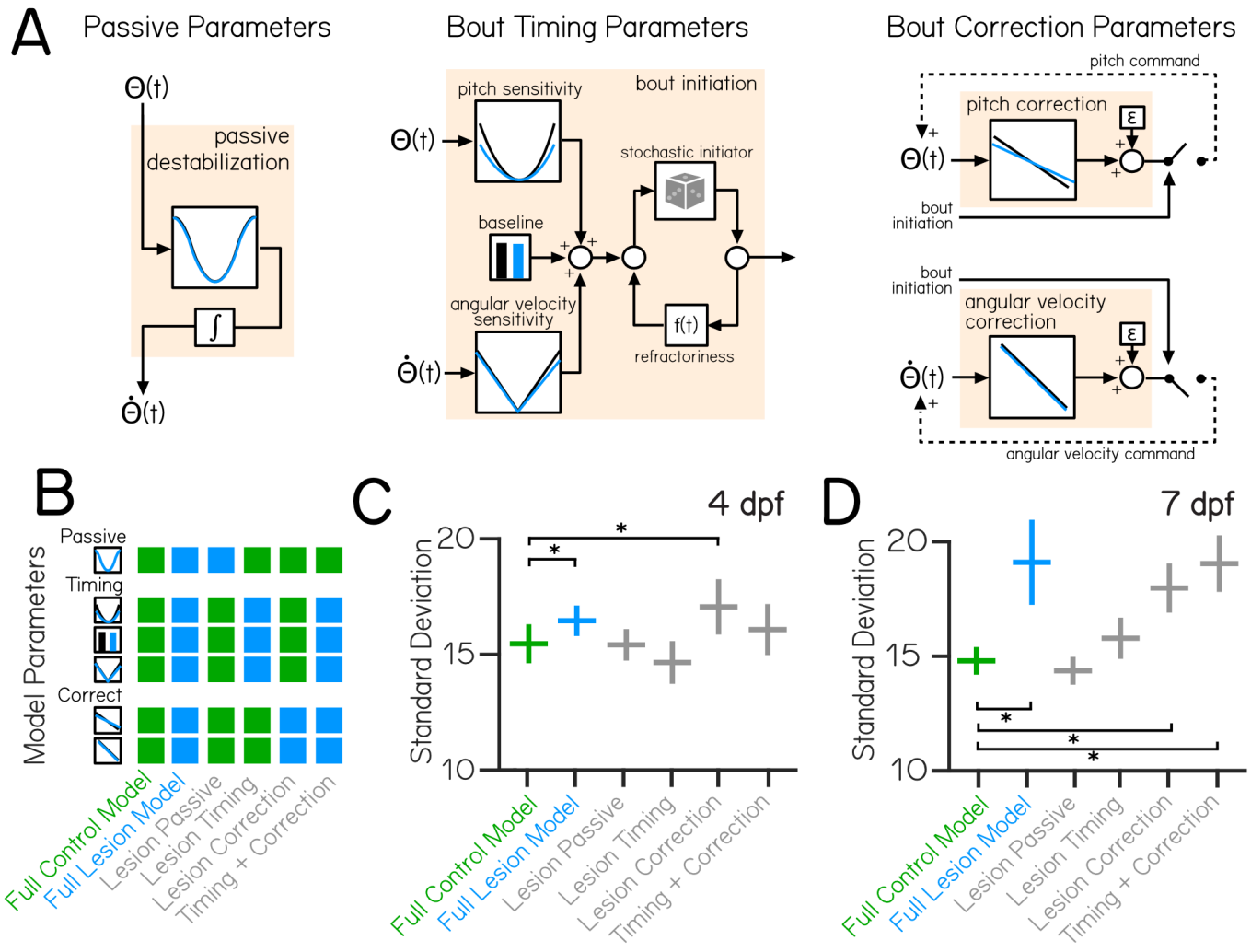

Figure 3: Behavioral modeling shows that increased postural variability following lesions emerges from combined impairments to swim timing and corrective capacity.
(A) A generative model of swimming adapted from previously published work[29], consists of four computations (tan boxes) determining swim timing, pitch angle, and angular velocity. Each computation contains one or more condition-specific parameters, shown by plots with a black (control) or blue (vestibulospinal lesion) line.
(B) Variations of the swimming model were created using parameters either entirely from control data ("Full Control Model", green), lesion data ("Full Lesion Model", blue), or combinations of parameters from control and lesion data ("Hybrid Models", gray).
(C) Standard deviation of simulated pitch probability distributions ±S.D. using different combinations of condition-specific parameters based on empirical data from 4 dpf or
(D) 7 dpf. Asterisks represent statistically significant differences, $p<0.05$.

As zebrafish larvae swim, they can change depth (i.e. swim up/down) in the water column. Depth change can be achieved through thrust-based or lift-based mechanisms[31,41]. When fish swim, they generate thrust that propels them in the direction they are facing – if the fish is at a non-horizontal posture, that thrust will result in a change in depth (Figure 4A, Thrust Δ Depth). Additionally, the pectoral fins can generate a vertical lift force to raise the fish. Pectoral fin loss eliminates all but thrust-based depth changes[41]. We estimate the depth change due to lift during a bout (Figure 4A, Lift Δ Depth) as the difference between the total experienced depth change (Figure 4A, Total Δ Depth) and the change in depth due to thrust (Thrust Δ Depth). The fins' contribution to depth changes can be described by the lift gain, defined as the slope of the linear relationship between Total Δ Depth and Lift Δ Depth. Lift gain is 1 when the change in depth can be explained entirely by lift, and a near-zero lift gain occurs when depth changes are not correlated with the generated lift (Figure 4A). If vestibulospinal neurons are involved in generating fin-based lift as larvae climb, loss of these neurons should reduce lift gain.

Lift gain was not affected by vestibulospinal lesions in the *Tg(nefma::EGFP)* line at 4 dpf (0.39±0.03 controls vs 0.40±0.03 lesioned, p=0.35). In contrast, at 7dpf, vestibulospinal lesions significantly reduced lift gain (0.46±0.02 controls vs 0.40±0.02 lesioned, $p=2.8\times10^{-21}$) (Figures 4B and 4C). Lift gain was also decreased in *Tg(α-tubulin:C3PA-GFP)* lesioned fish at 7 dpf, though this just failed to reach statistical significance (0.31±0.04 controls vs 0.28±0.03 lesioned, p=0.055). A decrease in lift gain in lesioned fish could arise due to an inability to use the fins to generate lift broadly. However,

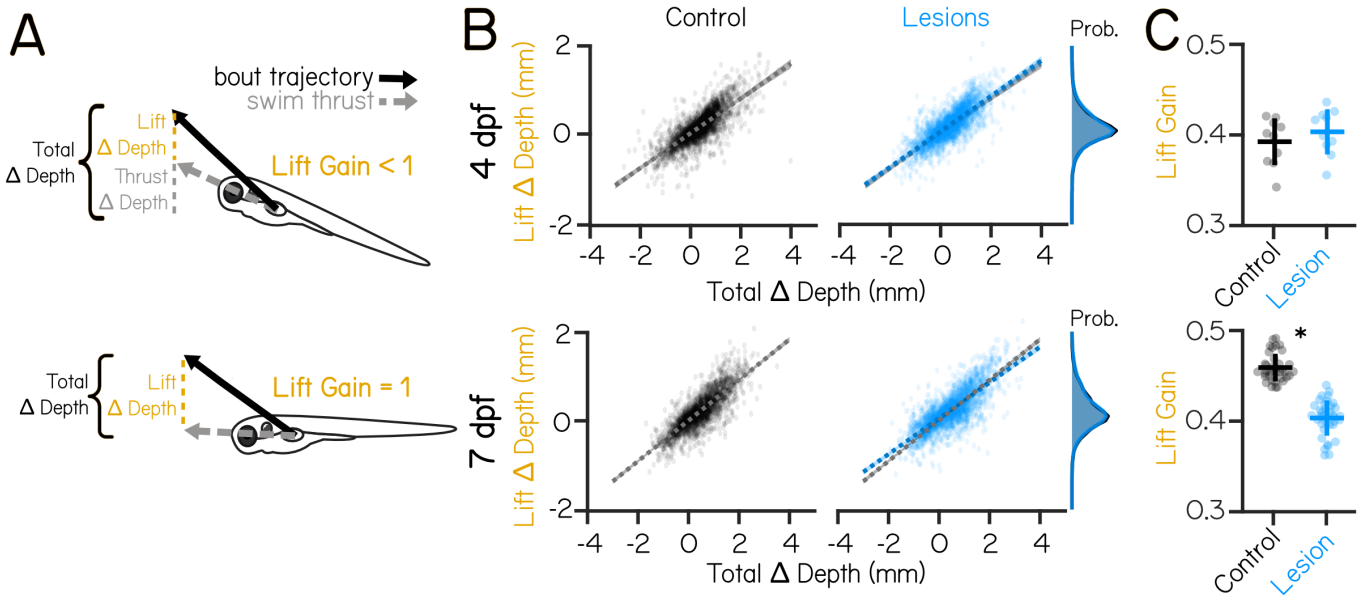

Figure 4: Vestibulospinal lesions disrupt fin and body coordination during vertical navigation only in older larvae
(A) Total depth change that occurs during swim bouts (Total Δ Depth, black) is the sum of depth change due to swim thrust in the direction the fish is pointing (Thrust Δ Depth, gray), and depth change due to vertical lift generated by the fins (Lift Δ Depth, yellow). Lift gain describes the strength of the relationship between Lift Δ Depth and Total Δ Depth.
(B) Estimated Lift Δ Depth as a function of the observed Total Δ Depth during a swim bout for control (black, left) and vestibulospinal lesioned (blue, right) fish at 4 dpf (top row) and 7 dpf (bottom row). Dots are single bouts, dashed lines are linear fits ± 1 SD. Control linear fits (gray) are replotted onto lesioned fish data for ease of comparison. Probability distributions (far right) show distribution of Lift Δ Depth across all total depth changes for lesioned fish (blue) and control fish (black) at 4 and 7 dpf.
(C) Lift gain in lesioned fish and sibling controls at 4 dpf (top) and 7 dpf (bottom). Lines are jackknifed mean ± 1 S.D., dots are jackknifed replicates. Asterisks represent statistically significant differences, $p<0.05$.

we observed that the distribution of all estimated lift magnitudes is comparable between lesioned fish and controls (Figure 4B) indicating that lesioned fish can produce fin-based lift of comparable magnitude. A lower lift gain could also result if lift is not coordinated strongly with the overall depth change of the bout. In support of this idea, we saw that lesioned fish had more antagonistic (negative depth change paired with positive lift) swim bouts than control fish at 7 dpf (7.6% of control bouts vs 10.3% of lesion bouts) but not at 4 dpf (7.3% of control bouts vs 7.6% of lesion bouts).

Larval zebrafish with vestibulospinal lesions at 7 dpf, but not 4 dpf, are impaired at coordinating fin-based lift with the appropriate body posture. We conclude that as fish develop, vestibulospinal neurons come to synergize fin and body movements to ensure effective climbs.

DISCUSSION

Vestibulospinal neurons are an evolutionarily ancient population long thought to play a role in balance regulation. Here we use the larval zebrafish as a model to define the contribution of these neurons to posture control and to understand how that contribution changes over early development. Targeted lesions show that acute loss of vestibulospinal neurons leads to postural instability in the pitch axis. Importantly, this instability is more pronounced in older larvae. Detailed analysis of free-swimming behavior after lesions revealed two failure modes: fish fail to initiate corrective swims appropriately, and their bouts do not adequately restore posture. Once again, the degree to which these balancing behaviors are impaired is age-dependent. *In silico,* inadequate corrective restoration explains increased postural variability after lesions at 4 dpf. However, it was necessary to incorporate both inadequate restoration and failures of swim initiation to explain variability at 7 dpf. Finally, we discovered that at 7 dpf, vestibulospinal neurons contribute to proper fin-body coordination, a key learned component of vertical navigation. Taken together, our data show that loss of vestibulospinal neurons at 7, but not 4 dpf, disrupts two key computations – swim initiation and fin-body coordination – that improve between 4 and 7 dpf[29,41]. Vestibulospinal-dependent behaviors therefore play increasingly important roles in postural stability. We conclude that the vestibulospinal nucleus is a locus of balance development in larval zebrafish. Vestibulospinal neurons are found in nearly all vertebrates. We propose that they serve as a partial substrate for a universal challenge: learning to stabilize posture during development.

Our lesion data and model argue that during locomotion vestibulospinal neurons partially facilitate two fundamental computations: specification of the degree of corrective movements and their timing. They do not appear to be necessary for determining postural set point or locomotor kinematics even though larvae can modulate both[29,44]. Similar findings were obtained following partial loss of homologous neurons in the lateral vestibular nucleus, which results in a reduction in the strength of corrective hindlimb reflexes following imposed destabilization[25,26]. Movement initiation (premature stepping) has been observed following stimulation of the lateral vestibular nucleus in cats[45,46], though

see[47]. This previous work was limited to animals that are restrained or performing a balance task; here we advance these studies by demonstrating detrimental impacts to corrective movement timing and gain in naturally-moving animals. Notably, unlike lesions of the vestibular periphery[41,48–50] neither our lesions nor comparable mammalian experiments produce gravity-blind animals, suggesting parallel means of postural control. Similar to observations in the lamprey[10,51], one parallel pathway likely involves a midbrain nucleus comprised of spinal-projecting neurons called the interstitial nucleus of Cajal, a.k.a. the nucleus of the medial longitudinal fasciculus (INC/nucMLF)[32,44,52–55]. Vestibular information reaches the INC/nucMLF through ascending vestibular neurons in the tangential nucleus[32,49,54,56]. Additionally, it is possible that information about body posture might derive from non-vestibular sensory feedback[57,58]. Taken together, our findings extend complementary loss- and gain-of-function experiments in vertebrates and define one part of the neural substrate for turning sensed imbalance into corrective behaviors.

In addition to regulating computations responsible for postural control, we discovered that loss of vestibulospinal neurons disrupts coordinated fin and body movements zebrafish use to navigate vertically in the water column. Considerable evidence indicates that pectoral fins are evolutionary predecessors to tetrapod forelimbs[43] that are driven by molecularly-conserved pools of motor neurons capable of terrestrial-like alternating gait[59]. Might vestibulospinal-mediated coordination of trunk and limbs be similarly conserved? Ancient vertebrates without paired appendages such as lampreys have homologous vestibulospinal neurons, but the projections of these neurons terminate in the most rostral portions of the spinal cord and have been postulated to be important in turning but less crucial for the maintenance of posture[10,60]. Vestibular-driven movements of the pectoral fin can be elicited in elasmobranches[61] and teleosts[32], indicating that some central vestibular pathway is directly or indirectly connected to the fins. Vestibulospinal neurons in frogs form a key part of the circuit that stabilizes posture at rest and coordinates trunk and hindlimb effectors for balance[62]. In terrestrial vertebrates, postural stability relies on coordination of “anti-gravity” extensor muscles in the trunk and limbs[63–66]. Mammalian vestibulospinal neurons innervate spinal regions that control both[7–9,38,67–69]. Intriguingly, subsets of vestibulospinal neurons in mice can have functionally different effects on balancing behaviors depending on their downstream spinal cord targets[26]. Evidence in zebrafish also supports the existence of subtypes of vestibulospinal neurons based on sensory afferent input and axon projection type[39]. A key challenge going forward will be identifying transcriptional determinants of subtype identity[70,71]; such a molecular atlas would allow for effective cross-species comparison of subtype function. Our finding that vestibulospinal neurons coordinate fin and trunk movements thus strengthens the proposal that the vestibulospinal circuit serves fundamentally similar roles across disparate body plans and locomotor strategies. By examining the function of vestibulospinal neurons across vertebrate species, we can speculate that vestibulospinal circuits evolved first to maintain posture through trunk effectors and were subsequently adapted to control and coordinate vestibular-drive movement of limbs/limb-like appendages.

As larval fish grow, vestibular-dependent computations involved in posture stabilization and navigation increase in strength[29,30,41]. Here, we identify the vestibulospinal nucleus as a locus for some of these vestibular-dependent computations We further demonstrate that the vestibulospinal contribution towards these computations increases with age. Specifically, loss of comparable numbers of vestibulospinal neurons had a significantly greater effect on behaviors assayed from 7-9 dpf than at 4-6 dpf. Increases to pitch sensitivity and pitch correction which normally occur between 4 and 7 dpf in non-lesioned fish were partially or entirely prevented by vestibulospinal lesion. We have therefore identified a substrate and a time window during which behaviorally-relevant circuit refinements likely occur. Notably, our findings do not require that physiological changes to the circuit happen within the vestibulospinal neurons themselves. Instead, they implicate changes within this sensorimotor circuit. Additionally, we note that while this study focused only on the effect of lesion at two time-points early in development, behavioral improvement continues until at least 3 weeks post-fertilization[29,41], meaning that functional refinement of posture circuits is not limited to only the window identified here. Increased ability to stabilize posture past 9 dpf (the latest timepoint studied here) may be due to increased contribution of vestibulospinal circuits, or to functional changes in other postural control circuits.

Though vestibulospinal neurons were first described over 150 years ago[72], they remain the focus of active interest today[25,26,34,36,57,62]. Here we examined the behavioral role of vestibulospinal neurons using precise loss-of-function perturbations with the comparatively simple and well-defined physics of underwater locomotion. We show that vestibulospinal neurons contribute to movement timing, corrective kinematics, and coordination between fin and trunk effectors during navigation. These behaviors are not only fundamental for proper posture and locomotion, but each improves with age[29,41]. The results here indicate that this developmental improvement resides, in part, within the sensorimotor transformation mediated by the vestibulospinal nucleus. Given the near ubiquity of vestibulospinal neurons across vertebrates, our findings are foundational for future studies into the neuronal mechanisms underlying vertebrate postural and locomotor development.

METHODS

Fish Care

All procedures involving zebrafish larvae (*Danio rerio*) were approved by the Institutional Animal Care and Use Committee of New York University. Fertilized eggs were collected and maintained at 28.5°C on a standard 14/10 hour light/dark cycle. Before 5 dpf, larvae were maintained at densities of 20-50 larvae per petri dish of 10 cm diameter, filled with 25-40 mL E3 with 0.5 ppm methylene blue. After 5 dpf, larvae were maintained at densities under 20 larvae per petri dish and were fed cultured rotifers (Reed Mariculture) daily.

Fish Lines

Experiments were done on the mitfa-/- background to remove pigment. Larvae for vestibulospinal lesions were labeled with the double transgenic *Tg(hsp70l:LOXP-RFP-LOXP-GAL4);Tg(UAS:EGFP)*, henceforth called *Tg(nefma::EGFP)*[36]. Photoconverted larvae used for additional vestibulospinal lesions were from the *Tg(α-tubulin:C3PA-GFP)*[49] background.

Labeling Vestibulospinal Neurons with Spinal Photoconversions

PA-GFP positive larvae were raised in a dark incubator to prevent background photoconversion. Larvae were anesthetized with 0.2 mg/mL ethyl-3-aminobenzoic acid ethyl ester (MESAB, Sigma-Aldrich E10521, St. Louis, MO) and mounted laterally in 2% low-melting temperature agarose (Thermo Fisher Scientific 16520). Using a Zeiss LSM800 confocal microscope with 20x objective (Zeiss W Plan-Apochromat 20x/1.0 DIC CG=0.17 M27 75mm), the spinal cord between the mid-point of the swim bladder and the caudal-most tip of the tail was repeatedly scanned with a 405 nm laser until fully converted. For retrograde labelling of vestibulospinal neurons used for photoablations, the spinal cords of *Tg(α-tubulin:C3PA-GFP)* larvae were converted at 6 dpf. To allow the converted fluorophore to diffuse into neuron bodies, all fish were removed from agarose after photoconversion and raised in E3 in a dark incubator.

Spinal Backfills

Spinal backfills were performed on some lesioned fish after behavioral assays were complete to confirm that vestibulospinal neurons had not regenerated during the behavioral window. To label spinal-projecting neurons in the hindbrain, larvae were anesthetized in 0.2 mg/mL MESAB and mounted laterally in 2% low-melting temperature agarose. Agarose was removed above the spinal cord at the level of the cloaca. An electrochemically sharpened tungsten needle (10130-05, Fine Science Tools, Foster City, CA) was used to create an incision in the skin, muscles, and spinal cord of the larvae. Excess water was removed from the incision site, and crystallized dye (dextran-conjugated Alexa Fluor 546/647 dye (10,000 MW, ThermoFisher Scientific D-22911/D-22914) was applied to the incision site using a tungsten needle. Larvae were left in agarose for at least 5 minutes after dye application before E3 was applied and the fish was removed from agarose. Fish were allowed to recover in E3 for 4-24 hours before imaging.

Vestibulospinal Photoablations

Vestibulospinal photoablations were performed on *Tg(nefma::EGFP)* larvae at either 4 dpf for use in behavioral experiments from 4-6 dpf, or at 6 or 7 dpf for use in behavioral experiments from 7-9 dpf. Additional experiments were performed on *Tg(α-tubulin:C3PA-GFP)* larvae after spinal photoconversion to target a larger number of vestibulospinal neurons. Larvae were anesthetized in 0.2 mg/ml MESAB and then mounted in 2% low-melting point agarose. Photoablations were performed on an upright microscope (ThorLabs) using a 80 MHz Ti:Sapphire oscillator-based laser at 920 nm for cell visualization (SpectraPhysics MaiTai HP) and a second, high-power pulsed infrared laser for two-photon mediated photoablation (SpectraPhysics Spirit 8W) at 1040 nm (200 kHz repetition rate, 500 pulse picker, 400 fs pulse duration, 4 pulses per neuron over 10 ms) at 25-75 nJ per pulse, depending on tissue depth. Sibling controls were anesthetized for matched durations to lesioned fish. Lesioned and control sibling larvae were allowed to recover for 4-24 hours post-procedure and were confirmed to be swimming spontaneously and responsive to acoustic stimuli before behavioral measurements.

Behavioral Measurement

Behavioral experiments were performed beginning at either 4 dpf or 7 dpf. For 4 dpf lesions, *Tg(nefma::EGFP)* experiments were performed on 54 vestibulospinal lesioned larvae, and 54 unlesioned sibling controls (5 paired clutch replicates). For 7 dpf lesions, *Tg(nefma::EGFP)* experiments were performed on 97 vestibulospinal lesioned larvae, and 76 unlesioned sibling controls (9 paired clutch replicates). *Tg(α-tubulin:C3PA-GFP)* experiments were performed on 17 vestibulospinal lesioned larvae, and 17 unlesioned sibling controls (5 paired clutch replicates) at 7 dpf. Larvae were filmed in groups of 1-8 siblings in a glass tank (93/G/10 55x55x10 mm, Starna Cells, Inc., Atascadero, CA, USA) filled with 24-26 mL E3 and recorded for 48 hours, with E3 refilled after 24 hours. Experiments were performed in constant darkness.

As described previously[29,41], video was captured using digital CMOS cameras (Blackfly PGE-23S6M, FLIR Systems, Goleta CA) equipped with close-focusing, manual zoom lenses (18-108 mm Macro Zoom 7000 Lens, Navitar, Inc., Rochester, NY, USA) with f-stop set to 16 to maximize depth of focus. The field-of-view, approximately 2x2 cm, was aligned concentrically with the tank face. A 5W 940nm infrared LED back-light (eBay) was transmitted through an aspheric condenser lens with a diffuser (ACL5040-DG15-B, ThorLabs, NJ). An infrared filter (43-953, Edmund Optics, NJ) was placed in the light path before the imaging lens. Digital video was recorded at 40 Hz with an exposure time of 1 ms. Kinematic data was extracted in real time using the NI-IMAQ vision acquisition environment of LabVIEW (National Instruments Corporation, Austin, TX, USA). Background images were subtracted from live video, intensity thresholding and particle detection were applied, and age-specific exclusion criteria for particle maximum Feret diameter (the greatest distance between two parallel planes restricting the particle) were used to identify larvae in each image. In each frame, the position of the visual center of mass and posture (body orientation in the pitch, or nose-up/down, axis) were collected. Posture was defined as the orientation, relative to horizontal, of the line passing through the visual centroid that minimizes the visual moment of inertia. A larva with posture zero at any given time has its longitudinal axis horizontal, while +90° is nose-up vertical, and -90° is nose-down vertical.

Behavioral Analysis

Data analysis and modeling were performed using Matlab (MathWorks, Natick, MA, USA). As previously described[29,41], epochs of consecutively saved frames lasting at least 2.5 sec were incorporated in subsequent analyses if they con-

tained only one larva. Instantaneous differences of body particle centroid position were used to calculate speed. Inter-bout intervals (IBIs) were calculated from bout onset times (speed positively crossing 5 mm/sec) in epochs containing multiple bouts, and consecutively detected bouts faster than 13.3 Hz were merged into single bouts.

Numerous properties of swim bouts were calculated. The maximum speed of a bout was determined from the largest displacement across two frames during the bout. Trajectory was calculated as the direction of instantaneous movement across those two frames. Displacement across each pair of frames at speeds above 5 mm/sec was summed to find net bout displacement. Bouts with backwards trajectories (>90° or <-90°) and those with displacements under 0.3 mm were excluded from analysis. Bout duration was calculated by linearly interpolating times crossing 5 mm/s on the rising and falling phases of each bout. Instantaneous bout rate was calculated as the inverse of the IBI duration. Pitch angle distributions were computed using inter-bout pitch, or the mean pitch angle across the duration of an IBI. Pitch probability distributions were calculated using a bin width of 5° (ranging from ±90°).

A parabolic function was used to fit the relationship between instantaneous bout rate (y) in Hz and deviation from preferred posture(x) in degrees, based on the formula

$$y(x) = sx^2 + b \tag{1}$$

in which s gives parabola steepness (pitch sensitivity, in Hz/deg^2) and b gives basal bout rate (Hz). Deviation from preferred posture was itself a function of inter-bout pitch, following the formula:

$$x = |\theta - p| \tag{2}$$

where θ is the inter-bout pitch (deg) and p is the mean inter-bout pitch across all IBIs for each condition. Parameter fits were estimated in Matlab using nonlinear regression-based solver (least-squares estimation). Initial parameter values were s=0.001 and b=1.

Net bout rotation was defined as the difference in pitch angle from 275 ms before to 75 ms after peak speed. Net change in angular velocity was defined as the difference in the mean angular velocity experienced from -225 to -125 ms (aligned to peak speed) and the mean angular velocity experienced from +250 to +375 ms. For both pitch correction gain and angular velocity gain, parameters were estimated in Matlab using Theil-Sen estimator.

Total depth change across a bout was calculated as the difference in the vertical position of the fish from 200 ms after peak speed to 250 ms before peak speed. Estimated depth change due to thrust was calculated as the product of the tangent of the fish's posture at the time of maximum linear acceleration of the swim bout and the empirical horizontal displacement of a bout from -250 to 200 ms aligned to peak speed. Estimated depth change due to lift was calculated ad the difference between total depth change and estimated depth change due to thrust.

Due to low bout numbers per experiment (704±366 bouts per clutch for 4 dpf experiments; 421 ± 277 bouts per clutch for 7 dpf *Tg(nefma::EGFP)* experiments), a single experiment often did not contain enough data to sufficiently sample the entire distribution of postures. Therefore data for all calculations were pooled across all bouts in a given group (lesion or control). Estimates of variation across clutches was performed using jackknifed resampling, where each sample left out two experimental clutch replicates. Statistics for behavioral measurements used jackknifed subsamples when the value being estimated was a parameter from a fit to a function or the standard deviation of the distributions, all other statistics were performed using experimental clutch replicates.

Behavioral Modeling

We generated condition-specific swimming simulations using a generative swim model described previously[29], with updates to the model to improve the fit to the empirical control dataset collected here. In each condition, 30 simulated fish swam for 3000 seconds with discrete time steps equivalent to those in the captured data ($\Delta t = 25$ ms). Pitch angle ($\Theta(t)$) is initialized at a randomly drawn integer from a uniform distribution between ±90°. At each time step (t), the pitch ($\Theta(t)$) is updated due to passive posture destabilization from the integral of angular velocity ($\dot{\Theta}$):

$$\Theta(t) = \Theta(t-1) + \dot{\Theta}(t)\Delta t \tag{3}$$

Angular velocity was initialized at 0, and was calculated as the sum of $\dot{\Theta}(t-1)$ and the integral of angular acceleration, $\ddot{\Theta}(t)$. Between swim bouts, simulated larvae were destabilized according to angular acceleration. Angular acceleration varied as a function of pitch in the preceding time step ($\Theta(t-1)$):

$$\ddot{\Theta}(t) = \ddot{\Theta}_c cos(\Theta(t-1)) \tag{4}$$

where $\ddot{\Theta}_c$ is a maximum angular acceleration for each inter-bout period randomly drawn from a normal distribution with a centered around $\ddot{\Theta}_p$ and with a spread of $\sigma_{\ddot{\Theta}}$, where $\ddot{\Theta}_p$ is the the median empirical angular acceleration observed between bouts for fish each condition, and $\ddot{\Theta}_p$ is the inter-quartile range of empirical angular acceleration between bouts.

Simulated larval pitch was updated across time according to passive destabilization until a swim bout was initiated. When a bout was initiated, pitch and angular velocity were updated according to condition-specific correction parameters based on empirical swim bout kinematics. Angular velocity correction from swim bouts was corrected by making

net angular acceleration across swim bouts ($\Delta\dot{\Theta}$) correlated with pre-bout angular velocity ($\dot{\Theta}_{pre}$). Condition-specific correlations were determined by a single best-fit line to empirical data, defined by a slope ($m_{\dot{\Theta}}$)and intercept ($b_{\dot{\Theta}}$). To reproduce the empirical variability of bout kinematics, net angular acceleration incorporated a noise term ($\varepsilon_{\Delta\dot{\Theta}|\dot{\Theta}_{pre}}$) drawn randomly from a Gaussian distribution with mean of 0, and standard deviation ($\sigma_{\Delta\dot{\Theta}}$) calculated from the empirical standard deviation of $\Delta\dot{\theta}$ and reduced proportionally by the unexplained variability from the correlation between $\Delta\dot{\Theta}$ and $\dot{\Theta}_{pre}$.

A bout initiated at time t corrected $\dot{\Theta}$ after completion of the bout, 100 ms later (4 time samples, matched to empirical bout duration):

$$\dot{\Theta}(t+4) = \dot{\Theta}(t) + m_{\dot{\Theta}}\dot{\Theta}(t) + b_{\dot{\Theta}} + \varepsilon_{\Delta\dot{\Theta}|\dot{\Theta}_{pre}} \tag{5}$$

The same approach was used to condition net bout rotation ($\Delta\Theta$) on pre-bout pitch (Θ_{pre}) based on a single best-fit line, with a single slope (m_{Θ} and intercept (b_{Θ}). For all conditions, the fit line was constrained to the linear portion of the relationship (-20 to +30° pre-bout pitch). If the simulated fish's posture prior to a bout was outside of this window (only 1% of simulated inter-bouts), net bout rotation was calculated using m_{-20}, b_{-20} if $\Theta < -20$, or m_{30}, b_{30} if $\Theta > 30$. To further impose a ceiling on the counter-rotation values attainable by our simulated larvae, a maximum net bout rotation was imposed ($\Delta\Theta_{max}$=±28.4°) based on empirical values; if $\Delta\Theta > \Delta\Theta_{max}$, then $\Delta\Theta$ was set to $\Delta\Theta_{max}$. As with angular velocity correction, net bout change also incorporated a noise term drawn from a randomly from a Gaussian distribution with a mean of 0, and a standard deviation (($\sigma_{\Delta\Theta}$) calculated from the empirical standard deviation of $\Delta\theta$ and reduced proportionally by the variability unexplained by the correlation.

Bouts occurred in the model based an internal state variable representing the probability of bout initiation (P_{bout}). Bout initiation was calculated as the sum of a non-posture dependent baseline bout rate variable (β), a Θ-dependent bout rate, and $\dot{\Theta}$-dependent bout rate:

$$P_{bout} = \beta_t + s(\Theta - p)^2 + r(\dot{\Theta} - c) \tag{6}$$

Bout rate as a function of pitch was calculated by fitting a parabola to the relationship between instantaneous bout rate and deviation from mean posture ($\Theta - p$) to get a pitch sensitivity parameter (s) for each condition. Bout rate as a function of angular velocity was calculated by fitting a line to the correlation between instantaneous bout rate and mean-subtracted angular velocity ($\dot{\Theta} - c$) to get a slope (r). Instantaneous bout rate increased linearly with the absolute value of ($\dot{\Theta} - c$); to account for this, two lines were fit to calculate two y-intercepts, one for negative values of ($\dot{\Theta} - c$) (b_{down}) and one for positive values (b_{up}). Baseline bout rate at a given time (β_t) was drawn from a random normal distribution with a mean (β) calculated from the mean y-intercept of the two best-fit lines and a spread (σ^{β}) equivalent to the standard error of β estimates. Lines were then re-fit to the data with y-intercepts fixed at β to calculate the slopes of the two best-fit lines (r_{down}, r_{up}).

Bout initiation probability was updated over time based on $\Theta(t)$ and $\dot{\Theta}(t)$, and was also made time-variant, with bout probability dropping to 0 in the first 100 ms (4 time samples) following a bout to match the empirical swim refractory period. After the 100 ms refractory period, swim probability increases to the full bout probability as a function of time elapsed from the last bout ($t - t_{bout}$):

(7)

Two parameters determined the shape and rise time of the time-dependency of P_{bout}: a time shift parameter, t_{shift} (in samples) and rise-time, τ (in samples). For each condition, these parameters were fit to minimize the difference between simulated inter-bout interval distribution with the empirical distribution.

To test that the modified version of swim simulation described here behaved in a similar manner to our previously published model[29], we compared our full model (described above) using parameters fit from control data with two null models with altered bout initiation and $\Theta/\dot{\Theta}$ bout correction terms in the model. In the "Bout Timing Null Model," bouts were initiated randomly in a pitch and angular velocity-independent manner:

$$P_{bout}(t) = \beta((1 - e^{\frac{-(t - t_{bout} - t_{shift})}{\tau}}) \tag{8}$$

In the "Bout Correction Null Model", Θ_{pre} and $\dot{\Theta}_{pre}$ were not correlated with $\Delta\Theta$ or $\Delta\dot{\Theta}$, and were instead drawn randomly from a Gaussian distribution with mean and standard deviation matched to empirical $\Delta\Theta$ or $\Delta\dot{\Theta}$ distributions. In the "Complete Null Model" both bout initiation and bout correction terms of the model were randomly drawn. Simulated bouts from the Bout Timing Null Model and Complete Null Model were less well balanced than the Full Model, and performed similarly to our previously published model (Figure S3A). To quantify the discriminability between the simulated pitch distributions of our full and null models and empirical pitch distributions from control larvae, we used the area under the receiver operating characteristic (AUROC). Non-overlapping distributions have an AUROC of 1 and identical distributions have an AUROC of 0.5. The comparison of the Full Control model to the empirical control data had an AUROC of 0.50 at 4 dpf and 0.43 at 7 dpf. The comparison of the Full Lesion model to the empirical lesion data had an AUROC of 0.57 at 4 dpf and 0.45 at 7 dpf.

To test the effects of vestibulospinal neuron lesions on pitch distributions of simulated larvae, we replaced subsets of parameters in the Full Control model with parameters fit from vestibulospinal lesion empirical data. In the Bout Timing model, $P_{bout}(t)$ was calculated using $\beta_{lesion}, s_{lesion}, r_{lesion}, t_{lesionshift}$, and τ_{lesion}, with all other parameters calculated from control data. In the Bout Correction model, $m_{\dot{\Theta}}, b_{\dot{\Theta}}, \epsilon_{\Delta\dot{\Theta}|\dot{\Theta}_{pre}}, m_{\Theta}, b_{\Theta}$, and $\epsilon_{\Delta\Theta|\Theta_{pre}}$ were replaced with parameters fit from lesion data, and all other computations calculated with control parameters. The comparison of the Full Lesion model to the empirical lesion data had an AUROC of 0.44. The Full Lesion Model was more stable than the empirical lesion data, capturing 71% of the postural variability (standard deviation) seen in the empirical vestibulospinal lesioned pitch distributions.

Statistics

The expected value and variance of data are reported as the mean and the standard deviation or the median and median absolute difference. When data satisfied criteria of normality, parametric statistical tests (t-tests) were used, otherwise we used their non-parametric counterparts. Unpaired statistics were used for comparisons between siblings, and paired (noted) tests used when comparing the same animals across time. To evaluate the bias in our estimates of the expected value (mean, median) we used a jacknife estimator that recomputed the expected value after leaving out one experimental repeat. Criteria for significance was set at α=0.05 and, when applicable, corrected for multiple comparisons.

Data sharing

All raw data and code for analysis are available at the Open Science Framework DOI 10.17605/OSF.IO/GVTHX.

ACKNOWLEDGMENTS

Research was supported by the National Institute on Deafness and Communication Disorders of the National Institutes of Health under award numbers R01DC017489 and F31DC019554. The authors would like to thank Martha Bagnall along with the members of the Schoppik and Nagel lab for their valuable feedback and discussions.

AUTHOR CONTRIBUTIONS

Conceptualization: KRH and DS, Methodology: KRH and DS, Investigation: KRH and KH, Resources: YK and SH, Visualization: KRH, Writing: KRH, Editing: DS, Funding Acquisition: KRH and DS, Supervision: DS.

AUTHOR COMPETING INTERESTS

The authors declare no competing interests.

REFERENCES

1. N.A. Bernshteĭn. *The Co-ordination and Regulation of Movements*. Pergamon Press, 1967.
2. H. J. Chiel, L. H. Ting, O. Ekeberg, and M. J. Z. Hartmann. The brain in its body: Motor control and sensing in a biomechanical context. *Journal of Neuroscience*, 29(41):12807–12814, October 2009.
3. J Massion and M Dufosse. Coordination between posture and movement: Why and how? *Physiology*, 3(3):88–93, June 1988.
4. M. H. Dickinson. How animals move: An integrative view. *Science*, 288(5463):100–106, April 2000.
5. Pieter Meyns, Sjoerd M. Bruijn, and Jacques Duysens. The how and why of arm swing during human walking. *Gait & Posture*, 38(4):555–562, September 2013.
6. S. Lund and O. Pompeiano. Monosynaptic excitation of alpha motoneurones from supraspinal structures in the cat. *Acta Physiologica Scandinavica*, 73(1-2):1–21, May 1968.
7. V J Wilson and M Yoshida. Comparison of effects of stimulation of deiters' nucleus and medial longitudinal fasciculus on neck, forelimb, and hindlimb motoneurons. *Journal of Neurophysiology*, 32(5):743–758, September 1969.
8. V. J. Wilson, M. Yoshida, and R. H. Schor. Supraspinal monosynaptic excitation and inhibition of thoracic back motoneurons. *Experimental Brain Research*, 11(3):282–295, June 1970.
9. S. Grillner, T. Hongo, and S. Lund. The vestibulospinal tract. effects on alpha-motoneurones in the lumbosacral spinal cord in the cat. *Experimental Brain Research*, 10(1):94–120, 1970.
10. C. M. Rovainen. Electrophysiology of vestibulospinal and vestibuloreticulospinal systems in lampreys. *Journal of Neurophysiology*, 42(3):745–766, May 1979.
11. Yunlu Zhu, Kyla R. Hamling, and David Schoppik. Vestibulospinal circuits and the development of balance in fish. In *The Senses: A Comprehensive Reference*, pages 326–333. Elsevier, 2020.
12. Richard Boyle. Vestibulo-spinal pathways in tetrapods. In *The Senses: A Comprehensive Reference*, pages 334–343. Elsevier, 2020.
13. O. Pompeiano and A. Brodal. The origin of vestibulospinal fibres in the cat. an experimental-anatomical study, with comments on the descending medial longitudinal fasciculus. *Archives Italiennes de Biologies*, 95:166–195, 1957.
14. M. Ito, T. Hongo, M. Yoshida, Y. Okada, and K. Obata. Intracellularly recorded antidromic responses of deiters' neurones. *Experientia*, 20(5):295–296, May 1964.
15. Fred Walberg, David Bowsher, and Alf Brodal. The termination of primary vestibular fibers in the vestibular nuclei in the cat. an experimental study with silver methods. *The Journal of Comparative Neurology*, 110(3):391–419, December 1958.
16. B W Peterson. Distribution of neural responses to tilting within vestibular nuclei of the cat. *Journal of Neurophysiology*, 33(6):750–767, November 1970.
17. Y. Uchino, H. Sato, K. Kushiro, M. Zakir, M. Imagawa, Y. Ogawa, M. Katsuta, and N. Isu. Cross-striolar and commissural inhibition in the otolith system. *Annals of the New York Academy of Sciences*, 871(1 Otolith Funct):162–172, May 1999.
18. Y Ogawa, K Kushiro, M Zakir, H Sato, and Y Uchino. Neuronal organization of the utricular macula concerned with innervation of single vestibular neurons in the cat. *Neuroscience Letters*, 278(1-2):89–92, January 2000.
19. V. H. Sarkisian. Input-output relations of deiters' lateral vestibulospinal neurons with different structures of the brain. *Archives Italiennes de Biologie*, 138(4):295–353, 2000.
20. G.N. Orlovsky. Activity of vestibulospinal neurons during locomotion. *Brain Research*, 46:85–98, November 1972.
21. G.N. Orlovsky and G.A. Pavlova. Response of deiters' neurons to tilt during locomotion. *Brain Research*, 42(1):212–214, July 1972.
22. R. H. Schor, A. D. Miller, and D. L. Tomko. Responses to head tilt in cat central vestibular neurons. i. direction of maximum sensitivity. *Journal of Neurophysiology*, 51(1):136–146, January 1984.
23. J. F. Fulton, E. G. T. Liddell, and D. Mcl. Rioch. The influence of unilateral destruction of the vestibular nuclei upon posture and the knee-jerk. *Brain*, 53(3):327–343, 1930.
24. C. D. Barnes and O. Pompeiano. The contribution of the medial and lateral vestibular nuclei to presynaptic and postsynaptic effects produced in the lumbar cord by vestibular volleys. *Pflugers Archiv European Journal of Physiology*, 317(1):1–9, 1970.

25. Maria Di Bonito, Jean-Luc Boulland, Wojciech Krezel, Eya Setti, Michèle Studer, and Joel C. Glover. Loss of projections, functional compensation, and residual deficits in the mammalian vestibulospinal system of hoxb1-deficient mice. *eneuro*, 2(6):ENEURO.0096–15.2015, November 2015.
26. Andrew J. Murray, Katherine Croce, Timothy Belton, Turgay Akay, and Thomas M. Jessell. Balance control mediated by vestibular circuits directing limb extension or antagonist muscle co-activation. *Cell Reports*, 22(5):1325–1338, January 2018.
27. R. McN. Alexander. *Functional Design in Fishes*. The Anchor Press, 1967.
28. Yuri Glebovich Aleyev. *Nekton*. Dr. W. Junk, 1977.
29. David E. Ehrlich and David Schoppik. Control of movement initiation underlies the development of balance. *Current Biology*, 27(3):334–344, feb 2017.
30. David E Ehrlich and David Schoppik. A novel mechanism for volitional locomotion in larval zebrafish. *bioRxiv*, sep 2017.
31. Yunlu Zhu, Franziska Auer, Hannah Gelnaw, Samantha N. Davis, Kyla R. Hamling, Christina E. May, Hassan Ahamed, Niels Ringstad, Katherine I. Nagel, and David Schoppik. SAMPL is a high-throughput solution to study unconstrained vertical behavior in small animals. *Cell Reports*, 42(6):112573, June 2023.
32. Takumi Sugioka, Masashi Tanimoto, and Shin ichi Higashijima. Biomechanics and neural circuits for vestibular-induced fine postural control in larval zebrafish. *Nature Communications*, 14(1), March 2023.
33. Charles B. Kimmel, Susan L. Powell, and Walter K. Metcalfe. Brain neurons which project to the spinal cord in young larvae of the zebrafish. *The Journal of Comparative Neurology*, 205(2):112–127, February 1982.
34. Kyla R. Hamling, Katherine Harmon, and David Schoppik. The nature and origin of synaptic inputs to vestibulospinal neurons in the larval zebrafish. *eneuro*, 10(6):ENEURO.0090–23.2023, June 2023.
35. Carmen Diaz and Joel C. Glover. The vestibular column in the mouse: A rhombomeric perspective. *Frontiers in Neuroanatomy*, 15, January 2022.
36. Zhikai Liu, Yukiko Kimura, Shin ichi Higashijima, David G.C. Hildebrand, Joshua L. Morgan, and Martha W. Bagnall. Central vestibular tuning arises from patterned convergence of otolith afferents. *Neuron*, 108(4):748–762.e4, November 2020.
37. Kyla R. Hamling, Yunlu Zhu, Franziska Auer, and David Schoppik. Tilt in place microscopy (TIPM): a simple, low-cost solution to image neural responses to body rotations. *The Journal of Neuroscience*, pages JN–RM–1736–22, December 2022.
38. Nedim Kasumacic, Joel C. Glover, and Marie-Claude Perreault. Segmental patterns of vestibular-mediated synaptic inputs to axial and limb motoneurons in the neonatal mouse assessed by optical recording. *The Journal of Physiology*, 588(24):4905–4925, December 2010.
39. Zhikai Liu, David G. C. Hildebrand, Joshua L. Morgan, Yizhen Jia, Nicholas Slimmon, and Martha W. Bagnall. Organization of the gravity-sensing system in zebrafish. *Nature Communications*, 13(1), August 2022.
40. Yizhen Jia and Martha W. Bagnall. Monosynaptic targets of utricular afferents in the larval zebrafish. *Frontiers in Neurology*, 13, July 2022.
41. David E Ehrlich and David Schoppik. A primal role for the vestibular sense in the development of coordinated locomotion. *eLife*, 8, October 2019.
42. Avinash Pujala and Minoru Koyama. Chronology-based architecture of descending circuits that underlie the development of locomotor repertoire after birth. *eLife*, 8, February 2019.
43. Neil H. Shubin, Edward B. Daeschler, and Farish A. Jenkins. The pectoral fin of tiktaalik roseae and the origin of the tetrapod limb. *Nature*, 440(7085):764–771, April 2006.
44. Kristen E. Severi, Ruben Portugues, João C. Marques, Donald M. O'Malley, Michael B. Orger, and Florian Engert. Neural control and modulation of swimming speed in the larval zebrafish. *Neuron*, 83(3):692–707, August 2014.
45. David F. Russell and Felix Zajac. Effects of stimulalating deiters' nucleus and medial longitudinal fasciculus on the timing of the fictive locomotor rhythm induced in cats by DOPA. *Brain Research*, 177(3):588–592, November 1979.
46. Hugues Leblond, Ariane Ménard, and Jean-Pierre Gossard. Bulbospinal control of spinal cord pathways generating locomotor extensor activities in the cat. *The Journal of Physiology*, 525(1):225–240, May 2000.
47. G.N. Orlovsky. The effect of different descending systems on flexor and extensor activity during locomotion. *Brain Research*, 40(2):359–372, May 1972.
48. Weike Mo, Fangyi Chen, Alex Nechiporuk, and Teresa Nicolson. Quantification of vestibular-induced eye movements in zebrafish larvae. *BMC Neuroscience*, 11(1):110, 2010.
49. Isaac H. Bianco, Leung-Hang Ma, David Schoppik, Drew N. Robson, Michael B. Orger, James C. Beck, Jennifer M. Li, Alexander F. Schier, Florian Engert, and Robert Baker. The tangential nucleus controls a gravito-inertial vestibulo-ocular reflex. *Current Biology*, 22(14):1285–1295, Jul 2012.
50. Richard Roberts, Jeffrey Elsner, and Martha W. Bagnall. Delayed otolith development does not impair vestibular circuit formation in zebrafish. *Journal of the Association for Research in Otolaryngology*, 18(3):415–425, March 2017.
51. T. G. Deliagina, G. N. Orlovsky, S. Grillner, and P. Wallén. Vestibular control of swimming in lamprey. ii. characteristics of spatial sensitivity of reticulospinal neurons. *Experimental Brain Research*, 90(3):489–498, September 1992.
52. Tod R. Thiele, Joseph C. Donovan, and Herwig Baier. Descending control of swim posture by a midbrain nucleus in zebrafish. *Neuron*, 83(3):679–691, August 2014.
53. Wei-Chun Wang and David L. McLean. Selective responses to tonic descending commands by temporal summation in a spinal motor pool. *Neuron*, 83(3):708–721, aug 2014.
54. Masashi Tanimoto, Ikuko Watakabe, and Shin ichi Higashijima. Tiltable objective microscope visualizes discrimination of static and dynamic head movement originates at hair cells. *Research Square*, July 2022.
55. Eva M. Berg, Leander Mrowka, Maria Bertuzzi, David Madrid, Laurence D. Picton, and Abdeljabbar El Manira. Brainstem circuits encoding start, speed, and duration of swimming in adult zebrafish. *Neuron*, 111(3):372–386.e4, February 2023.
56. David Schoppik, Isaac H. Bianco, David A. Prober, Adam D. Douglass, Drew N. Robson, Jennifer M.B. Li, Joel S.F. Greenwood, Edward Soucy, Florian Engert, and Alexander F. Schier. Gaze-stabilizing central vestibular neurons project asymmetrically to extraocular motoneuron pools. *The Journal of Neuroscience*, 37(47):11353–11365, sep 2017.
57. Emanuela Basaldella, Aya Takeoka, Markus Sigrist, and Silvia Arber. Multisensory signaling shapes vestibulo-motor circuit specificity. *Cell*, 163(2):301–312, October 2015.
58. Jeffrey Michael Hubbard, Urs Lucas Böhm, Andrew Prendergast, Po-En Brian Tseng, Morgan Newman, Caleb Stokes, and Claire Wyart. Intraspinal sensory neurons provide powerful inhibition to motor circuits ensuring postural control during locomotion. *Current Biology*, 26(21):2841–2853, November 2016.
59. Heekyung Jung, Myungin Baek, Kristen P. D'Elia, Catherine Boisvert, Peter D. Currie, Boon-Hui Tay, Byrappa Venkatesh, Stuart M. Brown, Adriana Heguy, David Schoppik, and Jeremy S. Dasen. The ancient origins of neural substrates for land walking. *Cell*, 172(4):667–682.e15, February 2018.
60. P. V. Zelenin, E. L. Pavlova, S. Grillner, G. N. Orlovsky, and T. G. Deliagina. Comparison of the motor effects of individual vestibulo- and reticulospinal neurons on dorsal and ventral myotomes in lamprey. *Journal of Neurophysiology*, 90(5):3161–3167, November 2003.
61. S.J.B. Timerick, D.H. Paul, and B.L. Roberts. Dynamic characteristics of vestibular-driven compensatory fin movements of the dogfish. *Brain Research*, 516(2):318–321, May 1990.
62. Anne Olechowski-Bessaguet, Raphaël Grandemange, Laura Cardoit, Elric Courty, François M. Lambert, and Didier Le Ray. Functional organization of vestibulospinal inputs on thoracic motoneurons responsible for trunk postural control in xenopus. *The Journal of Physiology*, 598(4):817–838, February 2020.
63. R H Schor and A D Miller. Vestibular reflexes in neck and forelimb muscles evoked by roll tilt. *Journal of Neurophysiology*, 46(1):167–178, July 1981.
64. J. Duysens, F. Clarac, and H. Cruse. Load-regulating mechanisms in gait and posture: Comparative aspects. *Physiological Reviews*, 80(1):83–133, January 2000.
65. Tatiana G. Deliagina, Irina N. Beloozerova, Ludmila B. Popova, Mikhail G. Sirota, Harvey A. Swadlow, Gunnar Grant, and Grigore N. Orlovsky. Role of different sensory inputs for maintenance of body posture in sitting rat and rabbit. *Motor Control*, 4(4):439–452, October 2000.
66. I. N. Beloozerova, P. V. Zelenin, L. B. Popova, G. N. Orlovsky, S. Grillner, and T. G. Deliagina. Postural control in the rabbit maintaining balance on the tilting platform. *Journal of Neurophysiology*, 90(6):3783–3793, December 2003.
67. D. M. Miller, D. A. Reighard, Amar S. Mehta, Ajeet S. Mehta, R. Kalash, and B. J. Yates. Responses of thoracic spinal interneurons to vestibular stimulation. *Experimental Brain Research*, 195(1):89–100, March 2009.
68. Bunya Kuze, Kiyoji Matsuyama, Toshihiro Matsui, Hideo Miyata, and Shigemi Mori. Segment-specific branching patterns of single vestibulospinal tract axons arising from the lateral vestibular nucleus in the cat: A PHA-l tracing study. *The Journal of Comparative Neurology*, 414(1):80–96, November 1999.

69. N. Kasumacic, F. M. Lambert, P. Coulon, H. Bras, L. Vinay, M.-C. Perreault, and J. C. Glover. Segmental organization of vestibulospinal inputs to spinal interneurons mediating crossed activation of thoracolumbar motoneurons in the neonatal mouse. *Journal of Neuroscience*, 35(21):8158–8169, May 2015.
70. Kristen P. D'Elia, Hanna Hameedy, Dena Goldblatt, Paul Frazel, Mercer Kriese, Yunlu Zhu, Kyla R. Hamling, Koichi Kawakami, Shane A. Liddelow, David Schoppik, and Jeremy S. Dasen. Determinants of motor neuron functional subtypes important for locomotor speed. *Cell Reports*, 42(9):113049, September 2023.
71. Irene Pallucchi, Maria Bertuzzi, David Madrid, Pierre Fontanel, Shin-ichi Higashijima, and Abdeljabbar El Manira. Molecular blueprints for spinal circuit modules controlling locomotor speed in zebrafish. *Nature Neuroscience*, November 2023.
72. Otto. Deiters and Max Johann Sigismund Schultze. *Untersuchungen über Gehirn und Rückenmark des Menschen und der Säugethiere / Nach dem Tode des Verfassers hrsg. von Max Schultze.* Vieweg„ 1865.

Table 1: Behavioral properties at 4 and 7 dpf

Variable	Unit	Control 4 dpf	Lesion 7 dpf	Control 4 dpf	Lesion 7 dpf
Med. Inter-bout interval (± S.D)	s	1.8 (±0.5)	1.6 (±0.2)	2.1 (±0.8)	1.6 (±0.4)
Med. Bout duration (± S.D)	s	0.13 (±0.01)	0.13 (±0)	0.12 (±0.02)	0.13 (±0.01)
Med. Bout displacement (± S.D)	mm	1.4 (±0.2)	1.3 (±0.1)	1.4 (±0.2)	1.5 (±0.2)
Maximum linear speed (± S.D)	mm/s	10.0 (±1.4)	9.6 (±0.7)	11.0 (±1.9)	11.3 (±1.8)

Table 2: Behavioral modeling parameters

Parameter	Symbol	Unit	Control 4 dpf	Lesion 4 dpf	Control 7 dpf	Lesion 7 dpf
Median angular acceleration	$\ddot{\Theta}_p$	deg/s^2	-0.43	-0.22	-1.1	-1.1
IQR angular acceleration	$\sigma_{\ddot{\Theta}}$	deg/s^2	11.5	11.7	8.5	10.3
Time-dependence shift	t_{shift}	seconds	-8750	-8750	-7500	-7500
Rise-time	τ	samples	8750	8750	8750	8750
Baseline bout rate	β	Hz	0.52	0.58	0.45	0.57
Baseline bout rate S.E.M	σ_β	Hz	0.55	0.57	0.64	0.62
Pitch sensitivity	s	mHz/deg^2	0.20	0.24	0.46	0.14
Pitch sensitivity S.E.M	σ_s	mHz/deg^2	0.02	0.02	0.03	0.01
AV sensitivity (down)	r_{down}	deg^{-1}	0.052	0.060	0.113	0.082
AV sensitivity (up)	r_{up}	deg^{-1}	0.069	0.077	0.058	0.057
AV sensitivity (down) S.E.M.	r_{down}	deg^{-1}	0.003	0.004	0.004	0.004
AV sensitivity (up) S.E.M.	r_{up}	deg^{-1}	0.003	0.003	0.004	0.004
Mean posture	p	deg	9.6	10.2	10.5	10.7
Mean angular velocity	c	deg/s	-0.7	0.3	-0.2	-0.8
Pitch correction gain	m_Θ	-	-0.25	-0.24	-0.34	-0.27
Net Bout Rotation S.D.	$\sigma_{\Delta\Theta}$	deg	7.5	8.0	8.9	9.1
Pitch correction R^2	-	-	0.45	0.40	0.52	0.43
AV correction gain	$m_{\dot{\Theta}}$	-	-0.98	-0.96	-0.96	-0.94
Net Angular Velocity Change S.D.	$\sigma_{\Delta\dot{\Theta}}$	deg/s	22.1	23.7	25.7	22.8
AV correction R^2	-	-	0.99	0.98	0.99	0.97

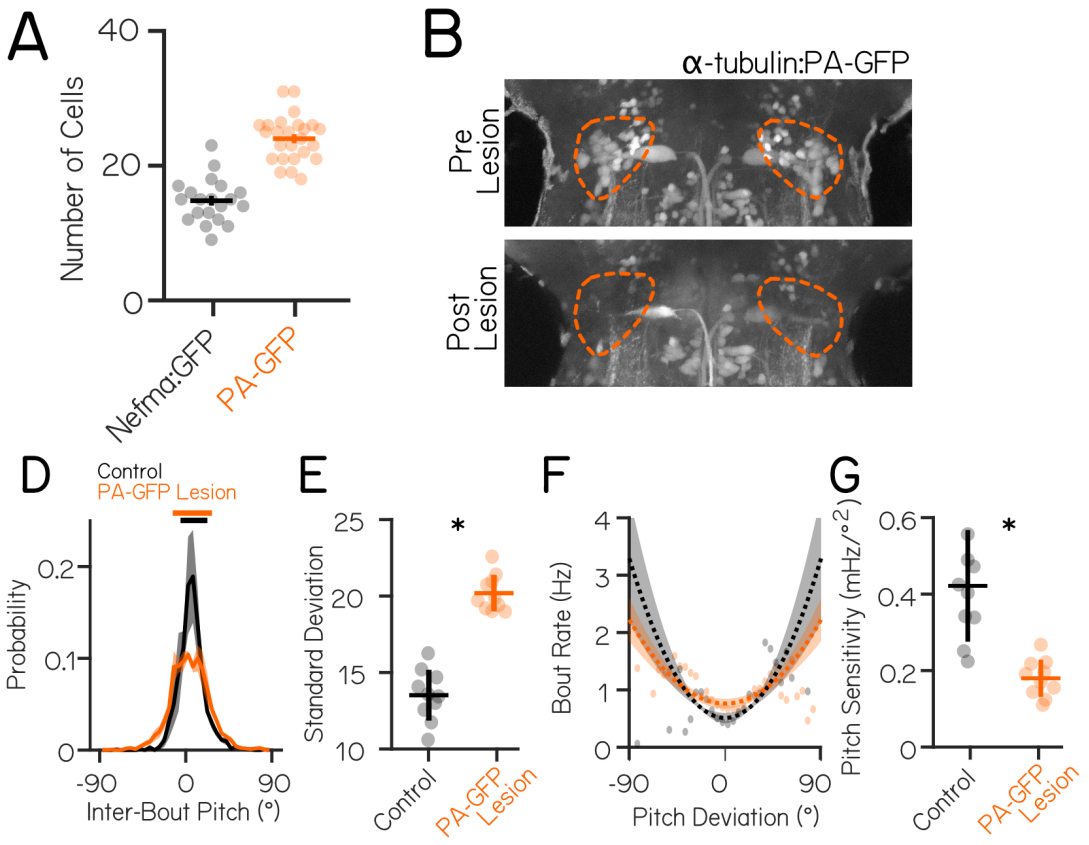

Figure S1: Lesions of a larger pool of vestibulospinal neurons at 7 dpf replicates postural disruption observed in *Tg(nefma::EGFP)* lesions. (A) *Tg(nefma::EGFP)* labels fewer (14.8 ± 0.7, n=20 hemispheres, 10 fish) neurons than optically-backfilled *Tg(α-tubulin:C3PA-GFP)* fish (24 ± 0.6, n=25 hemispheres, 13 fish, unpaired t-test $p=8.3x10^{-12}$).
(B) Dorsoventral distribution of vestibulospinal cells in both lines. *Tg(nefma::EGFP)* labels fewer cells in the dorsal vestibulospinal nucleus compared to photofills in *Tg(α-tubulin:C3PA-GFP)*.
(C) Representative maximum intensity projection of spinal projecting neurons in the hindbrain of a *Tg(α-tubulin:C3PA-GFP)* fish following optical backfill before (top) and after (bottom) two-photon mediated photoablation.
(D) Average probability distributions (± S.D) of inter-bout pitch angle for sibling controls (black, N=17 fish) and vestibulospinal lesioned fish (orange, N=17 fish) show no change in average posture (dashed vertical lines) but greater variability (solid horizontal lines ± 1 S.D.).
(E) Standard deviation of pitch is higher in vestibulospinal lesioned fish (20.2±1.2°) compared to sibling controls (13.5 ±1.7°, unpaired t-test $p=5.5x10^{-9}$).
(F) Bout rate as a function of deviation from preferred posture for lesions (orange) and control siblings (black). Solid lines represent raw data, dashed lines represent parabolic fits to raw data ± S.D. of the fit estimates.
(G) Pitch sensitivity (parabolic fit) is decreased in vestibulospinal lesioned fish (0.18 ± 0.05, unpaired t-test $p=9.9x10^{-5}$) compared to sibling controls (0.42 ± 0.15).

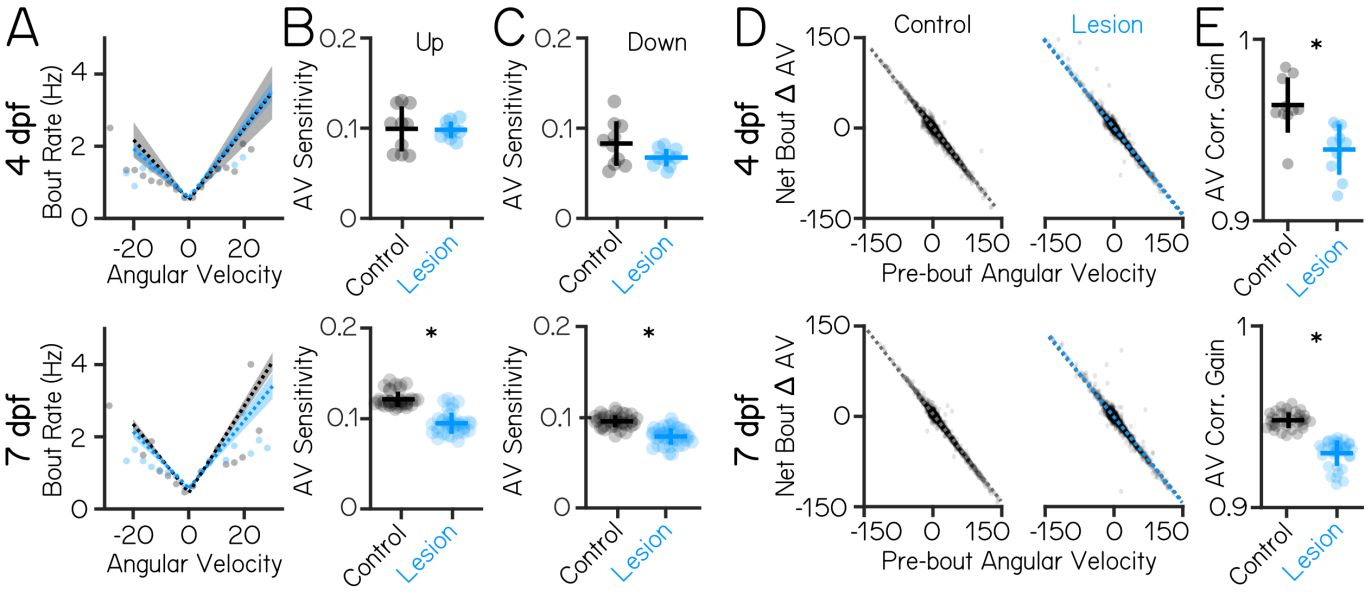

Figure S2: Vestibulospinal lesioned fish have disrupted angular velocity sensitivity and angular velocity correction. (A) Instantaneous bout rate as a function of angular velocity during inter-bout periods in vestibulospinal lesioned (blue) and control siblings (black) at 4 and 7 dpf. Dashed lines represent linear fits to raw data constrained to up and down angular velocities ±. 1 S.D. of fit estimates. Dots represent binned means of raw data in 3°/s wide bins.
(B) Angular velocity (AV) sensitivity (magnitude of linear slope fit) for lesioned and control fish for nose-up and
(C) nose-down angular velocities.
(D) Net change in angular velocity from the beginning to end of a swim bout as a function of pre-bout angular velocity. Dashed lines represent linear fits to raw data for lesioned (blue, right) or control (black, left) fish. Dots are raw data across all fish.
(E) Angular velocity correction gain (magnitude of linear slope fit) for lesioned and control fish at 4 and 7 dpf. Dots in panels B, C, and E are jackknifed estimates, lines are mean ± 1 S.D. of jackknifed estimates. Asterisks represent statistically significant effects, $p<0.05$.

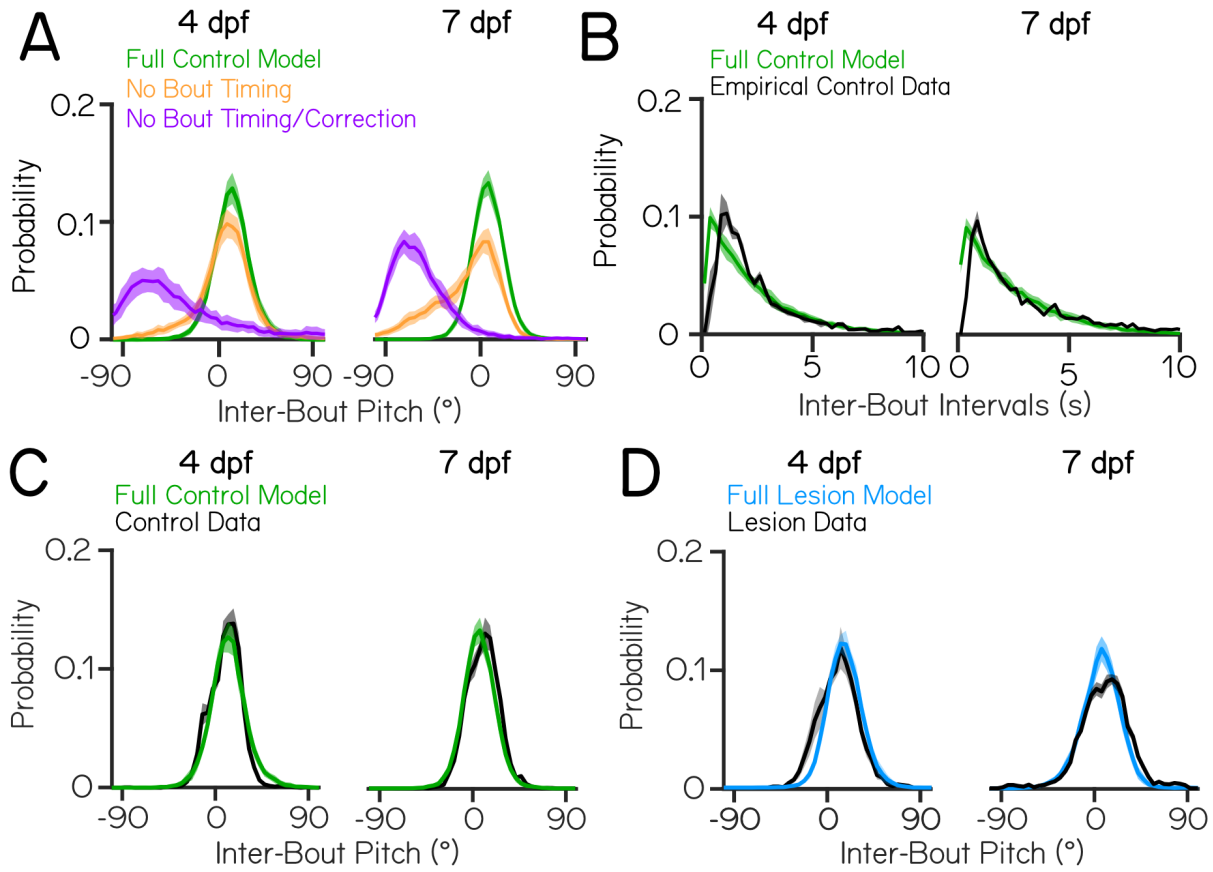

Figure S3: A model of zebrafish swimming during development generates bouts with expected pitch and event-frequency distributions. (A) Probability distributions of simulated pitch angles in full control model (green), bout timing null model (purple), and full null model (orange) are comparable for modeling data from 4 and 7 dpf, and are comparable to previous models of larval swimming [29].
(B) Probability distributions of simulated inter-bout intervals for empirical control data (black) and simulated control fish (green) using parameters derived from 4 and 7 dpf sibling control swimming datasets.
(C) Probability distributions of observed inter-bout pitch angles at 4 and 7 dpf for empirical control data (black) and simulated control fish (green) and
(D) empirical lesion data (black) and simulated lesion fish (blue)